29. Farde L, Hall H, Ehrin E, Sedvall G. Quantitative analysis of D2 dopamine receptor binding in the living human brain by PET. *Science* 1986;231:258–261.
30. Frost JJ, Douglass KH, Mayberg HS, et al. Multicompartmental analysis of [C-11]carfentanil binding to opiate receptors in humans measured by positron emission tomography. *J Cereb Blood Flow Metab* 1989;9:398–409.
31. Carson RE, Channing MA, Blasberg RG, et al. Comparison of bolus and infusion methods for receptor quantitation: application to [F-18]cyclofoxy and positron emission tomography. *J Cereb Blood Flow Metab* 1993;13:24–42.
32. Laruelle M, van Dyck C, Abi-Dargham A, et al. Compartmental modeling of iodine-123-iodobenzofuran binding to dopamine D2 receptors in healthy subjects. *J Nucl Med* 1994;35:743–754.
33. Nadeau SE, Couch MW, Devane L, Shukla SS. Regional analysis of D2 dopamine receptors in Parkinson's disease using SPECT and iodine-123-iodobenzamide. *J Nucl Med* 1995;36:384–393.
34. Kim SE, Lee WY, Chi DY, et al. SPECT imaging of dopamine transporter with [^{123}I] β-CIT: a potential clinical tool in Parkinson's disease. *Korean J Nucl Med* 1996;30: 19–34.
35. Kim HJ, Zeeberg BR, Reba RC. Theoretical investigation of the estimation of relative regional neuroreceptor concentration from a single SPECT or PET image. *IEEE Trans Med Imaging* 1990;9:247–261.
36. Marek KL, Seibyl JP, Zoghbi SS, et al. [I-123]β-CIT SPECT imaging demonstrates bilateral loss of dopamine transporters in hemi-Parkinson's disease. *Neurology* 1996;46:231–237.
37. van Dyck CH, Seibyl JP, Malison RT, et al. Age-related decline in striatal dopamine transporter binding with iodine-123-β-CIT SPECT. *J Nucl Med* 1995;36:1175–1181.
38. Mozley PD, Kim H-J, Gur RC, et al. Iodine-123-IPT SPECT imaging of CNS dopamine transporters: nonlinear effects of normal aging on striatal uptake values. *J Nucl Med* 1996;37:1965–1970.
39. Tatsch K, Schwarz J, Mozley PD, et al. Relationship between clinical features of Parkinson's disease and presynaptic dopamine transporter binding assessed with [I-123]IPT and SPECT. *Eur J Nucl Med* 1997: in press.

Iodine-123-Epidepride-SPECT: Studies in Parkinson's Disease, Multiple System Atrophy and Huntington's Disease

Walter Pirker, Susanne Asenbaum, Sylvia Wenger, Johannes Kornhuber, Peter Angelberger, Lüder Deecke, Ivo Podreka and Thomas Brücke

University Clinics for Neurology and Nuclear Medicine, Vienna, Austria; Department of Psychiatry, University of Göttingen, Göttingen, Germany; and Forschungszentrum Seibersdorf, Seibersdorf, Austria

Epidepride is a benzamide derivative with very high affinity for D2 receptors, which, in its [^{123}I]-labeled form, can be used for SPECT. The aim of this study was to evaluate the usefulness and accuracy of [^{123}I]epidepride-SPECT for the differential diagnosis of movement disorders. **Methods:** SPECT imaging with a triple-headed scintillation camera was performed in 9 patients with Parkinson's disease, 9 patients with probable multiple system atrophy (MSA), 1 patient with progressive supranuclear palsy, 16 patients with Huntington's disease (HD) and 14 controls, 3 hr after the intravenous injection of 3.7 ± 1.3 mCi of [^{123}I]epidepride. The striatum-to-cerebellum ratio − 1, reflecting the specific-to-nondisplaceable binding ratio, was used as a semiquantitative measure of D2 receptor binding. **Results:** Kinetic studies showed peak striatal uptake about 3 hr postinjection and a slow decline thereafter. The striatum-to-cerebellum ratio − 1 was significantly reduced in MSA (11.8 ± 3.9, compared to controls, 19.0 ± 6.3; $p < 0.01$) and in patients with HD (8.8 ± 3.2; $p < 0.00005$) but normal in Parkinson's disease (15.8 ± 3.6; not significant). A high interindividual variation of specific striatal epidepride binding (striatum − cerebellum; cpm/mCi × kg) was found in controls and in all patient groups. The interindividual variation of striatum-to-cerebellum ratios was lower but still considerable. In half of the MSA patients, the specific-to-nondisplaceable binding ratio fell within the range of controls. The use of various cortical reference regions did not improve discrimination between MSA and controls or Parkinson's disease patients, respectively. The discrimination of HD patients from controls was better, with overlap in only two cases. In one HD patient, calculation of the striatum-to-cerebellum ratio was almost impossible due to extremely low nonspecific binding. Possible explanations for the large variation of the ratios, resulting in an overlap between controls and different patient groups, are very low counting rates in the reference region and the fact that a transient binding equilibrium may not be achieved after bolus injection of epidepride. **Conclusion:** Epidepride appears to be a useful SPECT ligand for studying dopamine D2 receptors. However, its markedly higher specific-to-nondisplaceable binding ratio in comparison to those of iodobenzamide or other D2 ligands did not result in a better discrimination between different basal ganglia disorders. The calculation of plasma input curves and volumes of distribution might improve the accuracy of [^{123}I]epidepride-SPECT.

Key Words: dopamine; D2 receptors; epidepride; SPECT; basal ganglia disorders

J Nucl Med 1997; 38:1711–1717

Since the early 1980s, in vivo imaging of the postynaptic side and, more recently, of the presynaptic side of the nigrostriatal dopaminergic system has contributed significantly to our understanding of a variety of neuropsychiatric disorders. Dopamine D2 receptors have been studied with PET using butyrophenone derivatives such as [^{11}C]N-methylspiperone (*1*) and substituted benzamides like [^{11}C]raclopride (*2*). The first D2 receptor imaging study with SPECT was performed using [^{77}Br]spiperone (*3*). Because of their almost irreversible binding to D2 receptors, imaging studies with spiperone derivatives cannot be performed at equilibrium, and receptor binding can only be determined by performing dynamic studies and complicated mathematical calculations (*4*). The introduction of the benzamide [^{123}I]iodobenzamide (IBZM), which allowed imaging under pseudoequilibrium conditions and semiquantification with a simple ratio method using SPECT, led to a broader clinical application of D2 receptor imaging (*5–7*). Iodine-123-IBZM-SPECT was shown to be an effective tool for the differential diagnosis of Parkinson's disease and parkinsonism related to other neurodegenerative disorders, such as multiple system atrophy (MSA) and progressive supranuclear palsy (*8–12*) and drug-induced parkinsonism (*7,13–15*). However, IBZM has certain disadvantages as a SPECT ligand for D2 receptors; with a K_D of ~0.4 n*M* (*16,17*), the affinity for the D2 receptor is relatively moderate. Iodobenzamide is a highly

Received Nov. 7, 1996; revision accepted Mar. 11, 1997.
For correspondence or reprints contact: Walter Pirker, MD, Neurological University Clinic, Währinger Gürtel 18-20, A-1090 Vienna, Austria.

TABLE 1
Clinical Data

Subjects	n	Sex	Age (yr)		Disease duration (yr)		Hoehn and Yahr stage	
			Mean ± s.d.	Range	Mean ± s.d.	Range	Mean ± s.d.	Range
Control	14	6F, 8M	40.9 ± 13.3	19–63	—	—	—	—
Parkinson's disease	9	6F, 3M	65.0 ± 12.6	51–81	5.4 ± 2.7	1–9	2.9 ± 1.2	1–4
MSA	9	5F, 4M	62.7 ± 9.5	50–78	3.9 ± 2.3	1–8	4.1 ± 0.7	3–5
PSP	1	1M	65	—	4	—	4	—
HD	16	8F, 8M	47.0 ± 14.9	24–73	4.9 ± 4.6	1–17	—	—

lipophilic compound (*5*). Both moderate affinity and high lipophilicity lead to a relatively low ratio of specific to nonspecific binding (~1.7) (*7*). Moreover, due to the moderate affinity of IBZM, D2 receptor measurement may be confounded by the effect of endogenous dopamine or L-Dopa treatment (*18–20*).

In the late 1980s, several new substituted benzamides with high affinity for D2 receptors were proposed as potential SPECT imaging agents (*21–24*). In vitro data suggested that the IBZM derivative epidepride, (S)-N-[(1-ethyl-2-pyrrolidinyl) methyl]−5-iodo-2,3-dimethoxybenzamide, might be an excellent ligand for D2 receptor imaging (*22,25,26*). Epidepride predominantly labels dopamine D2 receptors with an affinity of about 30 p*M* in striatal and cortical tissue of the postmortem human brain (*25,27*). A part of striatal epidepride binding, especially in the ventral striatum, was shown to be due to D3 receptors (*28*), and a low percentage of cortical binding is represented by adrenergic alpha-2 receptors (*25,26,29,30*). SPECT studies by Kessler et al. and previous studies by our group (*31–35*) demonstrated that epidepride produces high striatum-to-cerebellum ratios and might be useful for studying striatal and extrastriatal dopamine D2 receptors.

The aim of this study was to evaluate the usefulness of [^{123}I]epidepride-SPECT for the differential diagnosis of movement disorders examining normal controls and patients with Parkinson's disease, MSA, progressive supranuclear palsy (PSP) and Huntington's disease (HD) and to determine if the markedly higher ratio of specific to nonspecific binding in comparison to IBZM would lead to a more accurate differentiation between these disorders.

MATERIALS AND METHODS

Patients

Thirty-five patients with movement disorders (19 women and 16 men) and 14 controls (6 women and 8 men, aged 19–63 yr; mean age 40.9 yr) were examined. The patient group consisted of 9 patients with Parkinson's disease (aged 51–81 yr; mean age 65.0 yr), 9 patients with MSA (aged 50–78 yr; mean age 62.7 yr), 1 patient with PSP (aged 65 yr) and 16 patients with HD (aged 24–73 yr; mean age 47.0 yr). Table 1 shows clinical data of the patients examined. Patients with Parkinson's disease had a mean disease duration of 5.4 yr and were in Hoehn and Yahr stage 2.9 (mean). Eight Parkinson's disease patients displayed an asymmetric, one showed a symmetric rigid-akinetic syndrome, and all patients responded well to L-Dopa. One Parkinson's disease patient had a history of head injury 30 yr before the study. Magnetic resonance imaging (MRI) revealed a small frontobasal lesion, presumably due to this trauma. Patients with MSA were clinically diagnosed as having probable sporadic olivopontocerebellar atrophy (MSA of OPCA-type; n = 3) or striatonigral degeneration (MSA of SND-type; n = 6) according to the criteria of Quinn (*36*). Mean duration of disease was 3.9 yr. Parkinsonian symptomatology was staged Hoehn and Yahr 4.1 (mean) and was asymmetric in three and symmetric in six MSA patients. MRI was performed in all MSA patients and revealed cerebellar atrophy in all OPCA patients and in four of six SND patients. The PSP patient (disease duration, 4 yr) fulfilled all clinical criteria for diagnosis, including vertical up-and-down gaze palsy. Vascular PSP was excluded by a normal MRI scan. Duration of disease was 4.9 yr (mean) in HD patients. MRI (n = 6) or CT scan (n = 5) revealed no atrophy of the caudate nucleus in nine and marked caudate atrophy in two HD patients. In 11 patients, the family history was positive; in two patients, it was suspect; and in one patient, it was negative for HD. Family history was not available in two HD patients. Genetic testing was performed in one of the latter two cases and confirmed the diagnosis of HD.

The control group consisted of 14 volunteers (healthy subjects and patients with peripheral neurological disorders).

L-Dopa treatment was continued in Parkinson's disease and MSA patients receiving L-Dopa. All other drugs known or suspected to interact with dopamine receptor binding (dopamine agonists and antagonists, anticholinergics, amantadine and selegiline) were discontinued (for 2 wk in the case of neuroleptics and for 24 hr in the case of other drugs) for the SPECT study.

Synthesis and Radiolabeling

Unlabeled epidepride was synthesized in six steps from o-vanillin and S-(−)-N-ethyl-2-amino-methyl-pyrrolidine. Epidepride was transformed into the labeling precursor Bu_3Sn-epidepride by reaction with Bu_3Sn_2 and $Pd(PPh_3)_4$ in dry toluene, which was isolated and purified by normal phase (silica) preparative high-performance liquid chromatography (HPLC) and analyzed by nuclear magnetic resonance, mass spectroscopy and HPLC. Iodine-123-epidepride was prepared from the precursor by oxidative iododestannylation ([^{123}I]-NaI, CAT, pH 2, room temperature, 3 min), isolated and purified directly from the reaction mixture by reversed-phase HPLC. After evaporation, redissolution in physiological saline and sterile filtration, [^{123}I]epidepride was obtained in 83% ± 7% (n = 6) yield and specific activity of about 0.1 nmol/mCi. Radiochemical purity, determined by thin-layer chromatography and HPLC, was ≥98% and remained stable for >24 hr. The product demonstrated specific striatal binding in rats.

Data Acquisition and Analysis

The SPECT studies were performed using a triple-headed rotating scintillation camera with a transaxial resolution of 9 mm FWHM. Camera heads were equipped with medium-energy collimators. Iodine-123-epidepride (3.7 ± 1.3 mCi, or 130 ± 46 mBq; range, 81–226 MBq) was injected intravenously as a single bolus. To determine the optimal time for data collection, dynamic studies with 2–15 scans were performed in four control subjects and in four patients with HD. Because specific binding in the striatum (striatum − cerebellum; cpm/mCi × kg body weight) showed a maximum around 3 hr postinjection, the time between 180 and 200 min postinjection was used as standard acquisition time for further studies. One of the controls and two HD patients, in whom dynamic studies had been performed, had not been scanned at this

time interval. Results of these three subjects were, therefore, not included in the statistical analysis. The rotation times were 20 min for all data acquisitions starting up to 12 hr postinjection and 40 min for acquisitions starting more than 12 hr postinjection. For each scan, a total of 180 frames was collected in a step-and-shoot mode.

Cross-sections (3.5 mm thick), oriented parallel to the canthomeatal plane, were reconstructed by filtered backprojection (Butterworth filter, cutoff frequency 0.7; order 7) in 128 × 128 matrices. Attenuation correction was performed assuming uniform attenuation within an ellipse drawn around the head contour (attenuation coefficient = 0.120/cm).

For analysis of the data, irregular regions of interest (ROIs) were drawn with the help of a brain atlas in areas corresponding to the left and right striatum, thalamus, inferior laterotemporal cortex, laterofrontal cortex and occipital cortex and in both cerebellar hemispheres. Counts in striatal and temporal regions were calculated in several consecutive 3.5-mm thick axial slices, and the slices with the highest counting rate for each striatum and temporal region were used to avoid tilting errors. The two striatal and temporal regions, respectively, were pooled together, and the average counts/pixel were calculated. Values of both cerebellar ROIs in three consecutive axial slices were pooled together, and the average cerebellar counts were calculated. The target-to-reference region ratio − 1, reflecting the specific-to-nondisplaceable binding ratio, was used as a semiquantitative measure of D2 receptor binding. The cerebellum was assumed to represent nonspecific bound and free radioactivity and, therefore, was used primarily as a reference region. In addition, the frontal, occipital and temporal cortex were used as reference regions.

An asymmetry index between left and right striatal [^{123}I]epidepride binding was calculated as follows: {Average (left + right/2) striatum-to-cerebellum ratio − 1} − {Striatum-to-cerebellum ratio − 1 in the striatum with lower binding}/{Average striatum-to-cerebellum ratio − 1} × 100.

The study was approved by the local ethical committee, and informed consent was obtained from every subject examined.

Statistical Evaluation

Specific binding, as calculated by the subtraction of target from cerebellar counting rates, and target-to-reference region ratios − 1 obtained 3 hr postinjection were used for statistical analysis. Values of the patient with PSP were included in the MSA group. Differences between groups were evaluated using ANOVA. Values of $p < 0.05$ were considered significant. Results were expressed as mean ± s.d.

RESULTS

Kinetic Study

Epidepride showed region-specific uptake, with highest binding in the areas corresponding to the left and the right striatum. Clearly visible activity was evident in several extrastriatal regions (thalamus > temporal cortex > frontal cortex > occipital cortex > cerebellum). Striatal uptake occurred with peak values at about 120–150 min postinjection and a slow decline thereafter (Fig. 1A). Specific binding in the control subject most extensively studied (Fig. 1B) and in the majority of other subjects remained stable between 120 and 180 min postinjection Striatal activity, measured in one control subject 17.5 hr postinjection, amounted to about 70% of the peak activity. With decreasing activity in different extrastriatal regions, peak activities occurred earlier, and washout was more rapid. Because of the more rapid washout of cerebellar activity as compared to binding in the striatum, striatum-to-cerebellum ratios increased steadily with time and reached values of >100 more than 6 hr postinjection.

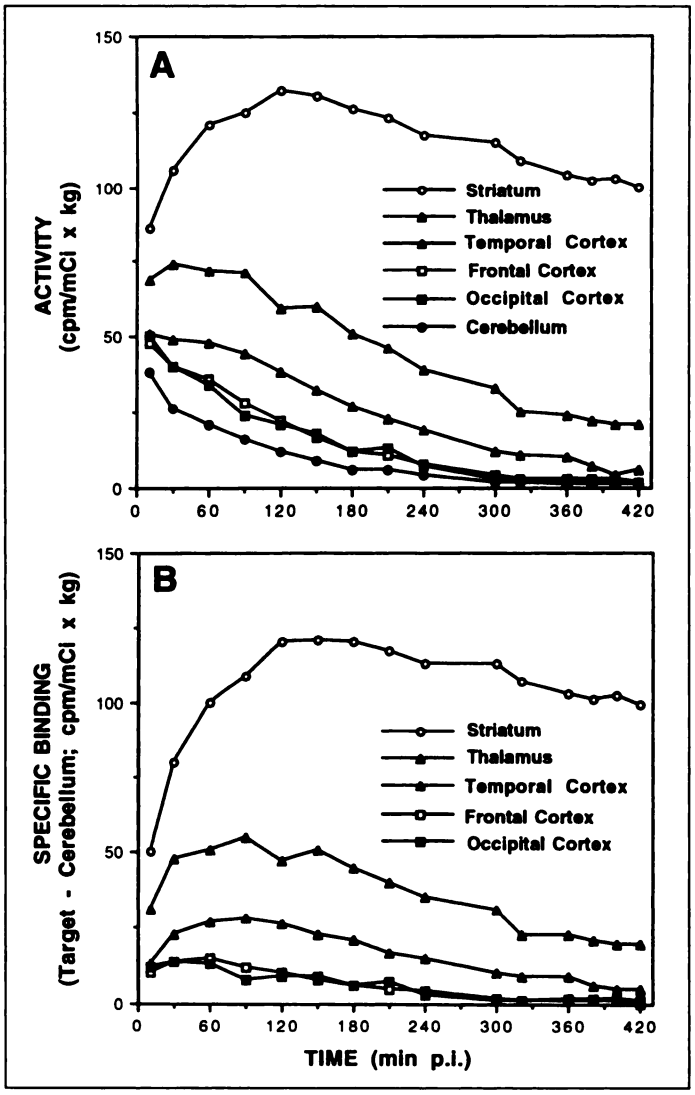

FIGURE 1. Time–activity distribution in a normal control after injection of 4 mCi of [^{123}I]epidepride. Activity curve shows highest binding in striatum, with peak uptake 120 min postinjection and a slow decline thereafter. With decreasing activity in different extrastriatal regions, peak activities occur earlier, and washout is more rapid (A). Specific striatal binding plateaus between 120 and 180 min postinjection (B). Radioactivity is expressed as mean counts/pixel/mCi × kg body weight. Specific binding is determined by subtraction of cerebellar activity from activity in different target regions.

A high interindividual variation of specific binding (cpm/mCi × kg) was found in controls and in all patient groups. The interindividual variation of striatum-to-cerebellum ratios of −1 was lower but still considerable.

Age Dependency

No significant age dependency of striatal epidepride binding (striatum-to-cerebellum ratios of −1) could be observed in normal controls [$r^2 = 0.04$, not significant (n.s.); Fig. 2].

Side-to-Side Differences in Striatal Epidepride Binding

Mean asymmetry indices of striatal epidepride binding 3 hr postinjection in controls and in the different patient groups are shown in Figure 3. There were no significant asymmetry differences between controls, Parkinson's disease, MSA and HD. The two hemiparkinsonian patients showed low asymmetry (0.4% and 0.7%). MSA patients with asymmetric disease showed a higher right-to-left difference than did patients with symmetric symptoms (mean, 5.6% compared to 2.2%), and in

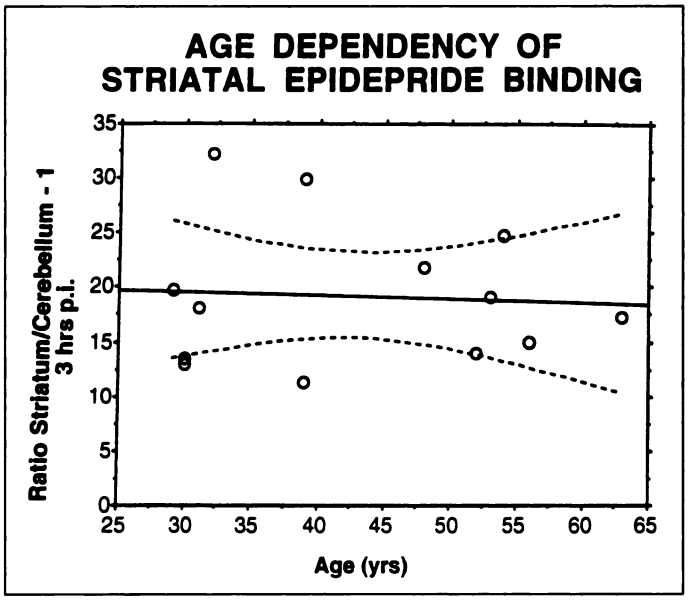

FIGURE 2. No age dependency of [^{123}I]epidepride binding (striatum-to-cerebellum ratios of −1) in the control group could be seen (r^2 = 0.04). Dotted lines indicate the 95% confidence intervals for the true mean of the ratios.

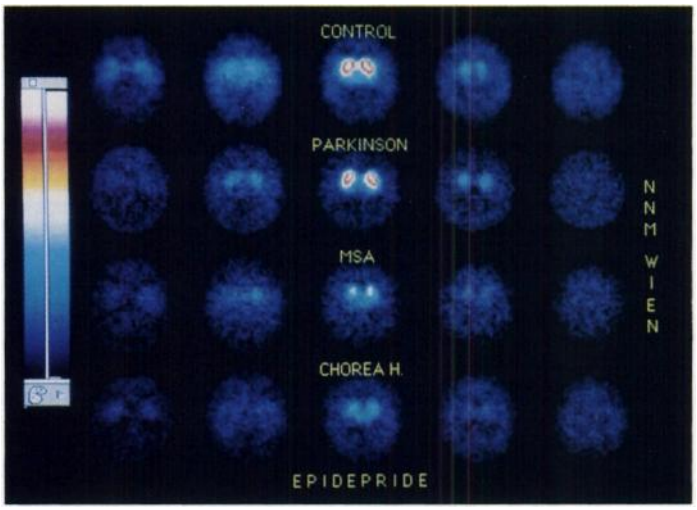

FIGURE 4. Iodine-123-epidepride-SPECT 3 hr postinjection in a control subject, a patient with Parkinson's disease, a patient with striatonigral degeneration (MSA of SND-type) and a patient with HD demonstrating normal striatal epidepride binding in the patient with Parkinson's disease and reduced binding in patients with MSA and HD. The four images are scaled to the maximum of the control. Axial SPECT-images (3.5-mm thick), each shifted by 17.5 mm beginning at the level of the cerebellum (left images). Maximal striatal binding is displayed on the middle images.

all three patients with asymmetric disease, striatal binding was lower opposite to the clinically more affected side.

Striatal Epidepride Binding in Parkinson's Disease, Multiple System Atrophy and Huntington's Disease

Figure 4 shows ^{123}I-epidepride binding in a control subject, a patient with Parkinson's disease, a patient with striatonigral degeneration and a patient with HD. Figure 5 demonstrates striatum-to-cerebellum and striatum-to-frontal, striatum-to-occipital and striatum-to-temporal cortex ratios 3 hr postinjection in each individual patient and control. The striatum-to-cerebellum ratio in Parkinson's disease patients as a group was not significantly different from controls (15.8 ± 3.6 compared to 19.0 ± 6.3, patients compared to controls; n.s.). One Parkinson's disease patient showed a striatum-to-cerebellum ratio below the range of controls (8.4). This patient had sustained a severe head injury 30 yr before the study.

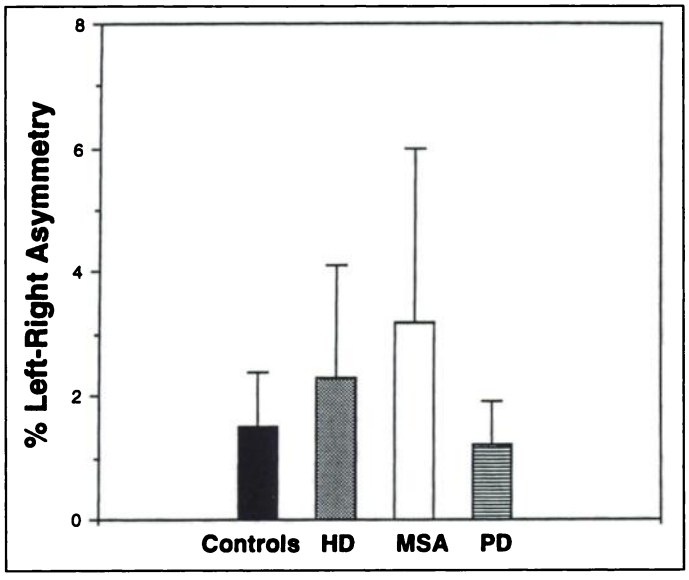

FIGURE 3. Asymmetry index of [^{123}I]-epidepride binding between left and right striatum in normal controls (n = 13) and patients with HD (n = 14), MSA (n = 10; including one patient with PSP) and Parkinson's disease (n = 9). No significant differences between groups were seen. Data are expressed as mean ± s.d.

The striatum-to-cerebellum ratios of −1 was significantly reduced in the MSA group as compared to controls (11.8 ± 4.9; $p < 0.01$; including, one PSP patient with a ratio of 8.5), but in half of the MSA patients, the ratio was within the range of controls. Difference of the striatum-to-cerebellum ratio between Parkinson's disease and MSA did not reach the level of significance. A highly significantly reduced striatum-to-cerebellum ratios of −1 was found in HD (8.8 ± 3.2; $p < 0.00005$), with little overlap with control values. In one HD patient, calculation of the striatum-to-cerebellum ratio was almost impossible due to extremely low binding in extrastriatal regions (ratio 18.0; mean cerebellar counts 1). The low injected dose (81 MBq) may have contributed to this result.

The use of frontal, occipital and temporal cortex did not prove to be superior to the use of the cerebellum as a reference region (Fig. 5). The striatum-to-frontal cortex ratios of −1 was significantly reduced in HD as compared to controls (5.6 ± 3.9 compared to 9.2 ± 3.0) and normal in Parkinson's disease (10.0 ± 1.9, n.s.). In MSA patients the striatum-to-frontal cortex ratio was neither different from controls nor from patients with Parkinson's disease (7.2 ± 2.3; n.s.). Similarly, striatum-to-occipital cortex ratios of −1 were significantly reduced in HD as compared to controls (5.8 ± 1.9 compared to 13.3 ± 4.3; $p < 00005$) but not different from controls in Parkinson's disease (13.8 ± 5.1; n.s.) and MSA (9.1 ± 1.9; n.s.). As demonstrated in the scatter diagram, there is an increased overlap between MSA patients and controls with only two patients below the range of controls using the occipital cortex as a reference region (Fig. 5). The striatum-to-temporal cortex ratio was found to be reduced in HD (2.4 ± 0.6 compared to 4.3 ± 1.1; HD compared to controls) and normal in Parkinson's disease patients (5.5 ± 1.3; n.s.). In MSA patients, the striatum-to-temporal cortex ratios of −1 was reduced as compared to patients with Parkinson's disease (4.1 ± 1.0; $p < 0.05$), but the difference from controls did not reach the level of significance.

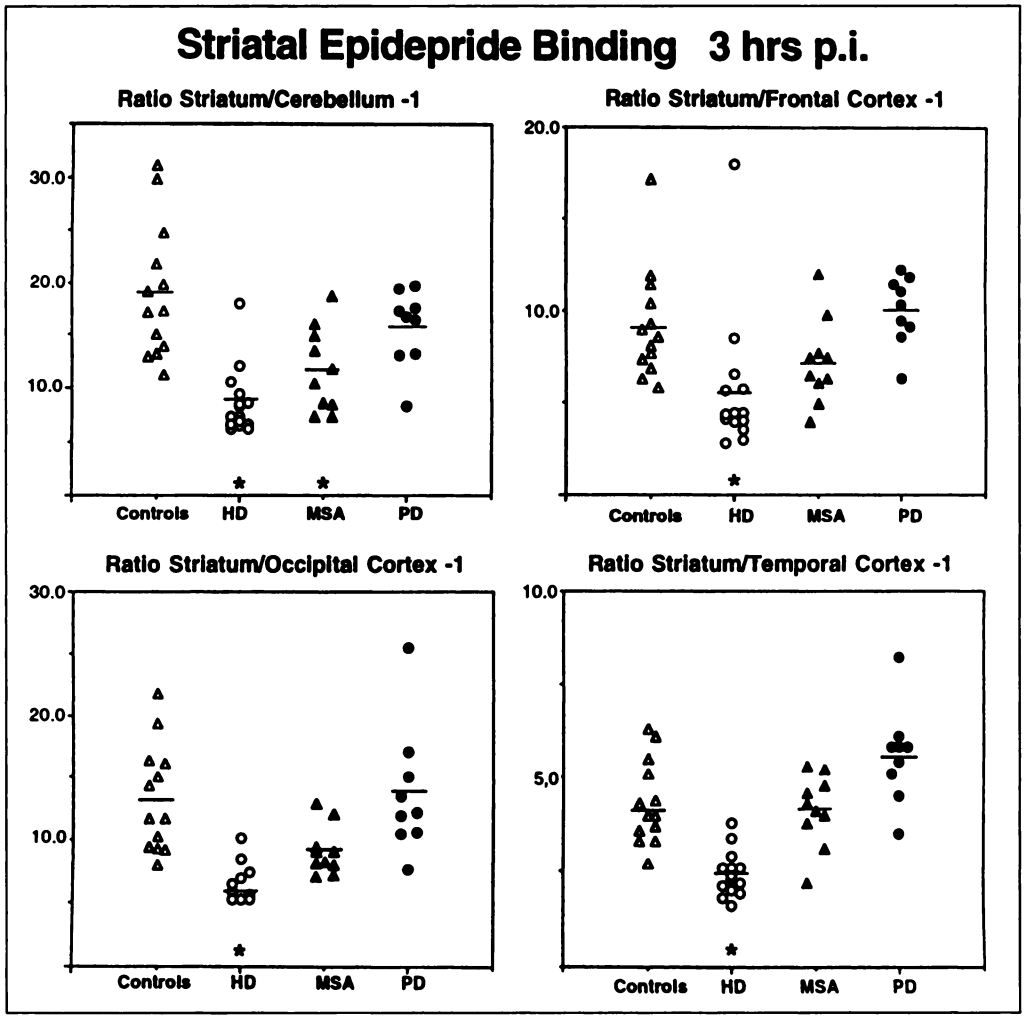

FIGURE 5. Striatum-to-reference region ratios 3 hr postinjection in normal controls (n = 13) and patients with HD (n = 14), MSA (n = 10; including one patient with PSP) and Parkinson's disease (n = 9). Significant differences in comparison to controls are given as $p < 0.05$ (*).

DISCUSSION

Recent reports demonstrated that epidepride, a novel substituted benzamide derivative with very high affinity for D2 receptors, can be used for studying striatal and extrastriatal dopamine D2 receptors in humans (*31–35*). This study has evaluated the usefulness of [^{123}I] epidepride and SPECT for the differential diagnosis of movement disorders.

In vitro data of epidepride binding demonstrated a very high affinity of this tracer to dopamine D2 receptors and also a very low nonspecific binding, which was thought to be due to its relatively low lipophilicity (*22*). It was suggested that a combination of these two features also would be advantageous for a receptor ligand for in vivo studies. At first glance, it would seem to be a clear-cut advantage to use a tracer with very high specific and low nonspecific binding, which increases the signal-to-noise ratio and offers the possibility of studying extrastriatal binding sites with low receptor density. In fact, it has been shown that [^{123}I]epidepride SPECT can visualize D2 receptors on different pituitary adenomas with high sensitivity not only in prolactinomas but also in clinically nonfunctioning and in growth hormone-producing adenomas (*37*). Due to its lower affinity and lower binding ratio, [^{123}I]IBZM has a much lower sensitivity to label D2 receptors on pituitary tumors in vivo (*38*).

This study shows that patients with HD, MSA and PSP are, as a group, significantly different and can be separated with [^{123}I]epidepride SPECT from controls but that this is not possible in individual cases due to a substantial overlap of the data, especially in the MSA group. This overlap could be due to the relatively large variation of the control values (coefficient of variation of striatal-to-cerebellar ratios 3 hr postinjection in this study = 33%) compared with a relatively small variation of IBZM binding ratios in normals reported in a previous study from our own group (coefficient of variation = 5%) (*10*). There are several reasons for the large variation of [^{123}I]epidepride binding ratios. One is the extremely low nonspecific binding of this tracer in the brain, which makes it difficult to delineate the cerebellum or other reference regions and causes a high uncertainty in the calculation of the ratios when the nonspecific binding in the denominator is very low. Because initial epidepride uptake corresponds to blood flow and peak uptake occurs earlier in cortical regions as compared to the striatum, the delineation of extrastriatal regions might be improved by performing an early scan in each patient in future studies. The anatomical information obtained with an early scan could be used for ROI placement in the later scan representing receptor distribution. Another reason for the variation of the data might be the fact that, after bolus injection of [^{123}I]epidepride, a transient equilibrium of tracer binding is not achieved. Ideally, in vivo receptor measurements should be performed in a state of true equilibrium when there are constant activity levels in plasma and all brain compartments, but this usually can only be achieved with constant infusion of the tracer (*39*). A constant relationship between the specific bound compartment in the brain and the metabolite corrected plasma input function has been termed "transient equilibrium." During such a transient equilibrium, the apparent volume of distribution of a tracer can be used as an index of receptor density (*39*). Such measure-

ments of the volume of distribution of a ligand require repeated measurements of its concentration in plasma and are difficult to perform in a clinical setting. A method to estimate the true equilibrium between specific and nonspecific binding has been proposed by Farde et al. (*2*), who used the time point of maximal specific binding of the D2 ligand raclopride for the calculation of the specific-to-nonspecific ratio. This approach also was used in this study. Kinetic data show a maximum of specific binding in striatum about 3 hr after injection with a slow decline thereafter (Fig. 1B). Therefore, this time was used as standard acquisition time. However, data of striatal specific binding show that there is probably some interindividual variation of the time course of tracer uptake, which contributes to the variation of the binding ratios.

In a similar study that used the D2 receptor ligand [^{123}I]IBF, which has about a fourfold higher affinity than IBZM, the differentiation of MSA and PSP patients from patients with Parkinson's disease was investigated (*40*). Pathophysiologically MSA and PSP differ from Parkinson's disease by the involvement of postsynaptic structures in the striatum, which also degenerate in these disorders and lead to a loss of postsynaptically-located D2 receptors. This is the pathophysiological background for the reduction of D2 receptor binding in the striatum in MSA and PSP. Buck et al. (*40*) also found an overlap of [^{123}I]IBF binding between normals and MSA and PSP patients. Thus, a less clear-cut separation was found than in previous studies with IBZM (*8–12*) despite the higher affinity and higher basal ganglia to frontal cortex ratio of IBF binding, which is very similar to our findings with [^{123}I]epidepride in this study.

It is well-established that D2 receptor binding decreases with increasing age (*7,15*). The fact that such an age-related decline of epidepride binding in controls is not seen here (Fig. 2) is probably also due to the large variation of the data. The use of different cortical regions (frontal, occipital or temporal cortex) as reference regions did not improve the separation of MSA patients from controls and Parkinson's disease patients. A better separation was found for the HD patients, perhaps because the pathology and neuronal loss in the striatum is more severe in these patients.

This study shows that high affinity and low nonspecific binding of epidepride, which makes it an ideal ligand for in vitro studies, did not lead to a better separation of MSA patients from patients with Parkinson's disease and controls. Other methods of quantification, such as the determination of the volume of distribution and the use of a bolus infusion technique (*39*) for the application of epidepride, might help to reduce the variation of the results and to take advantage of the large potential of this substance, especially for the measurement of extrastriatal D2 receptors.

CONCLUSION

Epidepride appears to be a suitable ligand for in vivo imaging of dopamine D2 receptors in basal ganglia disorders. The striatum-to-cerebellum ratios of −1 is about 25 times higher for epidepride than for IBZM (19.0 compared to 0.7). However, due to the high interindividual variation of binding in patients and in controls, this increase did not result in an improved accuracy in the discrimination between Parkinson's disease and parkinsonian syndromes in other neurodegenerative disorders. The large variation of the values might be due to imaging under nonequilibrium conditions and very low counting rates in the reference region.

REFERENCES

1. Wagner HN Jr, Burns HD, Dannals RF, et al. Imaging dopamine receptors in the human brain by positron tomography. *Science* 1983;221:1264–1266.
2. Farde L, Hall H, Ehrin E, Sedvall G. Quantitative analysis of D2 dopamine receptor binding in the living human brain by PET. *Science* 1986;231:258–261.
3. Crawley JCW, Smith T, Veall N, Zanelli GD, Crow TJ, Owen F. Dopamine receptor displayed in the living human brain with ^{77}Br-spiperone [Letter]. *Lancet* 1983;2:975P.
4. Wong DF, Gjedde A, Wagner HN Jr. Quantification of neuroreceptors in the living human brain. I. Irreversible binding of ligands. *J Cereb Blood Flow Metab* 1986;6: 137–146.
5. Kung HF, Pan S, Kung MP, Kasliwal R, Reilly J, Alavi A. In vitro and in vivo evaluation of [^{123}I]IBZM: a potential CNS D-2 dopamine receptor imaging agent. *J Nucl Med* 1989;30:88–92.
6. Kung HF, Alavi A, Chang W, et al. In vivo SPECT imaging of dopamine receptors: initial studies with iodine-123-IBZM in humans. *J Nucl Med* 1990;31:573–579.
7. Brücke T, Podreka I, Angelberger P, et al. Dopamine D2 receptor imaging with SPECT: studies in different neuropsychiatric disorders. *J Cereb Blood Flow Metab* 1991;11:220–228.
8. Tatsch K, Schwartz J, Oertel W, Kirsch CM. SPECT imaging of dopamine D2 receptors with I-123 IBZM in parkinsonian syndromes. *J Nucl Med* 1991;32:1014–1015.
9. Schwarz J, Tatsch K, Arnold G, et al. ^{123}I-iodobenzamide-SPECT predicts dopaminergic responsiveness in patients with de novo parkinsonism. *Neurology* 1992;42:556–561.
10. Brücke T, Wenger S, Asenbaum S, et al. Dopamine D2 receptor imaging and measurement with SPECT. *Adv Neurol* 1993;60:494–500.
11. van Royen EA, Verhoeff NPLG, Speelman JD, Wolters EC, Kuiper MA, Jansen AGM. Diminished striatal dopamine D2 receptor activity in multiple system atrophy and progressive supranuclear palsy, demonstrated by ^{123}I-IBZM SPECT. *Arch Neurol* 1993;50:513–516.
12. Schulz JB, Klockgether T, Petersen D, et al. Multiple system atrophy: natural history, MRI morphology, and dopamine receptor imaging with ^{123}I-IBZM-SPECT. *J Neurol Neurosurg Psychiatry* 1994;57:1047–1056.
13. Brücke T, Roth J, Podreka I, Strobl R, Wenger S, Asenbaum S. Striatal dopamine D2-receptor blockade by typical and atypical neuroleptics. *Lancet* 1992;339:497.
14. Pilowsky LS, Costa DC, Ell PJ, Murray RM, Verhoeff NPLG, Kerwin RW. Clozapine, single photon emission tomography and the D2 dopamine receptor blockade hypothesis of schizophrenia. *Lancet* 1992;340:199–202.
15. Brücke T, Wöber C, Podreka I, et al. D2 receptor blockade by flunarizine and cinnarizine explains extrapyramidal side effects. A SPECT study. *J Cereb Blood Flow Metab* 1995;15:513–518.
16. Brücke T, Tsai YF, McLellan C, et al. In vitro binding properties and autoradiographic imaging of 3-iodobenzamide ([^{125}I]-IBZM): a potential imaging ligand for D-2 dopamine receptors in SPECT. *Life Sci* 1988;42:2097–2104.
17. Kung HF, Kasliwal R, Pan S, Kng MP, Mach RH, Guo YZ. Dopamine D-2 receptor imaging radiopharmaceuticals: synthesis, radiolabeling, and in vitro binding of (R)-(+)- and (S)-(−)-3-iodo-2-hydroxy-6-methoxy-N-[(1-ethyl-2-pyrrolidinyl)methyl]benzamide. *J Med Chem* 1988;31:1039–1043.
18. Dewey SL, Logan J, Wolf AP, et al. Amphetamine induced decreases in (^{18}F)-N-methylspiroperidol binding in the baboon brain using positron emission tomography (PET). *Synapse* 1991;7:324–327.
19. Dewey SL, Smith GS, Logan J, Brodie JD, Fowler JS, Wolf AP. Striatal binding of the ligand ^{11}C-raclopride is altered by drugs that modify synaptic dopamine levels. *Synapse* 1993;13:350–356.
20. Innis RB, Malison RT, Al-Tikriti N, et al. Amphetamine-stimulated dopamine release competes in vivo for [^{123}I]IBZM binding to the D2 receptor in nonhuman primates. *Synapse* 1992;10:177–184.
21. Murphy RA, Kung HF, Billings JJ, Yang Y, Murphy RA, Alavi A. The characterization of IBF as a new selective dopamine D2 receptor imaging agent. *J Nucl Med* 1993;20:1146–1153.
22. Kessler RM, Ansari MS, de Paulis T, et al. High-affinity dopamine D2 receptor radioligands. 1. Regional rat brain distribution of iodinated benzamides. *J Nucl Med* 1991;32:1593–1600.
23. Hall H, Högberg T, Halldin C, et al. NCQ 298, a new selective iodinated salicylamide ligand for the labeling of dopamine D2 receptors. *Psychopharmacology* 1991;103:6–13.
24. Chumpradit S, Kung MP, Billings J, Mach R, Kung HF. Fluorinated and iodinated dopamine agents: D2 imaging agents for PET and SPECT. *J Med Chem* 1993;36:221–228.
25. Joyce JN, Janowsky A, Neve KA. Characterization and distribution of [125I]-epidepride binding to dopamine D2 receptors in basal ganglia and cortex of human brain. *J Pharmacol Exp Ther* 1991;257:1253–1263.
26. Kessler RM, Ansari MS, Schmidt DE, et al. High-affinity dopamine D2 receptor radioligands. 2. [^{125}I]epidepride, a potent and specific radioligand for the characterization of striatal and extrastriatal dopamine D2 receptors. *Life Sci* 1991;49:617–628.
27. Kessler RM, Whetsell WO, Ansari MS, et al. Identification of extrastriatal dopamine D2 receptors in postmortem human brain with [^{123}I] epidepride. *Brain Res* 1993;609: 237–243.
28. Murray AM, Ryoo H, Joyce JN. Visualization of dopamine D3-like receptors in human brain with [^{125}I] epidepride. *Eur J Pharmacol* 1992;227:443–445.
29. Neve KA, Henningsen RA, Kinzie JM, et al. Sodium-dependent isomerization of dopamine D-2 receptors characterized using [^{125}I] epidepride, a high-affinity substituted benzamide ligand. *J Pharmacol Exp Ther* 1990;252:1108–1116.
30. Janowsky A, Neve KA, Kinzie JM, Taylor B, de Paulis T, Belknap JK. Extrastriatal dopamine D2 receptors: distribution, pharmacological characterization and region-specific regulation by clozapine. *J Pharmacol Exp Ther* 1992;261:1282–1290.
31. Kessler RM, Mason NS, Votaw RJ, et al. Visualization of extrastriatal dopamine D2 receptors in the human brain. *Eur J Pharmacol* 1992;223:105–107.

32. Kessler RM, Votaw JR, Schmidt DE, et al. High-affinity dopamine D2 receptor radioligands. 3. [^{123}I] and [^{125}I]epidepride: in vivo studies in rhesus monkey brain and comparison with in vitro pharmacokinetics in rat brain. *Life Sci* 1993;53:241–250.
33. Pirker W, Brücke T, Kornhuber J, Asenbaum S, Angelberger P, Podreka I. D2 receptor measurement in striatum and extrastriatal areas with [I-123]-epidepride and SPECT [Abstract]. *Movement Disorders* 1994;9(suppl 1):116.
34. Kornhuber J, Brücke T, Angelberger P, Asenbaum S, Podreka I. SPECT imaging of dopamine receptors with [I-123]-epidepride: characterization of uptake in the human brain. *J Neural Transm* 1995;101:95–103.
35. Kessler RM, Mason NS, Ansari MS, et al. I-123 epidepride SPECT studies of dopamine D2 receptors in striatal and extrastriatal regions: effects of neuroleptic blockade [Abstract]. *J Nucl Med* 1995;36:88P.
36. Quinn N. Multiple system atrophy. In: Marsden CD, Fahn S, eds. *Movement disorders 3*. London: Butterworth–Heinemann; 1994:262–281.
37. Pirker W, Riedl M, Luger A, et al. Dopamine D2 receptor imaging in pituitary adenomas using [^{123}I]-epidepride and SPECT. *J Nucl Med* 1996;37:1931–1937.
38. Pirker W, Brücke T, Riedl M, et al. Iodine-123-IBZM-SPECT: studies in 15 patients with pituitary tumors. *J Neural Transm* 1994;97:235–244.
39. Carson RE, Channing MA, Blasberg RG, et al. Comparison of bolus and infusion methods for receptor quantification: application to [^{18}F]cyclofoxy and positron emission tomography. *J Cereb Blood Flow Metab* 1993;13:24–42.
40. Buck A, Westera G, Sutter M, Albani C, Kung HF, von Schulthess GK. Iodine-123-IBF SPECT evaluation of extrapyramidal diseases. *J Nucl Med* 1995;36:1196–1200.

Fluorine-18-FDG Evaluation of Crossed Cerebellar Diaschisis in Head Injury

Abass Alavi, Adam Mirot, Andrew Newberg, Wayne Alves, Theodore Gosfield, Jesse Berlin, Martin Reivich and Thomas Gennarelli

Division of Nuclear Medicine, Department of Neurology, University of Pennsylvania, Philadelphia, Pennsylvania

This study investigates the phenomenon of crossed cerebellar diaschisis in head injury patients. **Methods:** We visually compared fluorine-18-fluorodeoxyglucose (FDG)-PET images to radiograph computed tomography or magnetic resonance images in 19 patients with head injury. **Results:** We found that of 68 focal unilateral lesions, 40% were associated with contralateral cerebellar hypometabolism and 19% were associated with ipsilateral cerebellar hypometabolism. Of supratentorial, extraparenchymal lesions (n = 20), 45% were associated with contralateral cerebellar hypometabolism, whereas 15% had ipsilateral cerebellar hypometabolism. Intraparenchymal lesions were associated with contralateral cerebellar hypometabolism in 38% of the patients and with ipsilateral cerebellar hypometabolism in 21% of the patients. Of the cortical lesions that were the patients' most severe injury, 69% were associated with contralateral cerebellar hypometabolism, whereas only 8% were associated with ipsilateral cerebellar hypometabolism. In patients with focal supratentorial lesions alone, 50% of all focal lesions were associated with contralateral cerebellar hypometabolism and 13% had ipsilateral hypometabolism. Of patients with both focal and diffuse brain injuries, 27% of the focal lesions had contralateral cerebellar hypometabolism and 27% had ipsilateral cerebellar hypometabolism to the most severe focal injury. **Conclusion:** Crossed cerebellar diaschisis is seen more often in patients with focal cortical or extraparenchymal injuries and is not seen in patients with multiple or diffuse brain injuries. Furthermore, this predominance is more pronounced with lesions of the greatest severity.

Key Words: PET; head injury; cerebellar diaschisis

J Nucl Med 1997; 38:1717–1720

Since the advent of functional brain imaging, several studies using PET and SPECT have shown that lesions such as infarction and tumor in the cerebral cortex are associated with contralateral cerebellar hypometabolism or hypoperfusion (*1–9*). The evidence to support a similar pattern secondary to head trauma has been lacking in the literature. Studies have reported changes in regional blood flow and metabolism in areas remote from the original site of injury. We have reported both ipsilateral and contralateral cerebellar hypometabolism as the result of head trauma (*10,11*). This study reports a comprehensive analysis of fluorine-18-fluorodeoxyglucose (FDG)-PET studies performed on head trauma patients. Specifically, we have determined the presence and laterality of cerebellar hypometabolism in relation to primary lesions above the tentorium.

MATERIALS AND METHODS

All patients in this retrospective analysis were participants in an ongoing study of central nervous system abnormalities that accompany severe head injury. Twenty-nine patients (with no history of previous neurological disorder or head trauma) who sustained head injury severe enough to require hospitalization were enrolled in this study. Therefore, there were no inclusion or exclusion criteria for the analysis reported in this article. All patients underwent radiograph computed tomography (CT) and/or magnetic resonance imaging (MRI) and [^{18}F]FDG-PET imaging to determine the structural and functional consequences of head injury. Of the 29 patients, 22 were men and 7 were women. The subjects ranged in age from 18 yr to 59 yr with a mean age of 27 yr. Glasgow coma scores were assigned to each patient at the time of initial presentation to the emergency room. These scores ranged from 3 to 14 with a mean of 9 (15 represents complete consciousness and 3 denotes deep coma). Glasgow coma scores were also determined at the time of the PET scans; these scores ranged from 4 to 15 with a mean of 11.

CT images were obtained using a GE 8800 or GE 9800 CT scanner. Slices were obtained with a thickness of 5 mm in the majority of patients and no intravenous contrast was used. Magnetic resonance images were obtained using a GE 1.5 Tesla superconducting magnet and a multislice spin–echo technique. Axial images were generated with a pulse repetition time of 1500–2500 msec and two echoes (TE 25 and 120 msec) yielding mixed intensity and T-2 weighted images.

MRI and CT images of the brain were evaluated blindly by a neuroradiologist. However, no interior intrarater reliability was determined for either the anatomic or functional images. Anatomic lesions were identified and recorded. Focal lesions were categorized as one of the following: gunshot wound, cortical contusion, intracerebral hematoma, tissue tear hemorrhage, focal axonal damage, basal ganglia hemorrhage, secondary infarction, epidural hematoma, acute subdural hematoma, subacute subdural hema-

Received Sep. 16, 1996; revision accepted Feb. 24, 1997.
For correspondence or reprints contact: Abass Alavi, MD, Professor and Chief, Division of Nuclear Medicine, 117 Donner Building, H.U.P., 3400 Spruce St., Philadelphia, PA 19104.